Cellular Physiology and Biochemistry

Cell Physiol Biochem 2018;50:1376-1397
DOI: 10.1159/000494598
Published online: 25 October 2018
Accepted: 17 October 2018

Original Paper

Dynamic Methylation Changes of DNA and H3K4 by RG108 Improve Epigenetic Reprogramming of Somatic Cell Nuclear Transfer Embryos in Pigs

Yanhui Zhai[a,b] Zhiren Zhang[c] Hao Yu[c] Li Su[d] Gang Yao[d]
Xiaoling Ma[a] Qi Li[a] Xinglan An[a] Sheng Zhang[a] Ziyi Li[a]

[a]First Hospital, Jilin University, Changchun, [b]College of Veterinary Medicine, Jilin University, Changchun, [c]College of Animal Science, Jilin University, Changchun, [d]Second Hospital, Jilin University, Changchun, China

Key Words
Rg108 • SCNT embryos • DNA methylation • Epigenetic reprogramming • Pigs

Abstract
Background/Aims: DNA methylation and histone modifications are essential epigenetic marks that can significantly affect the mammalian somatic cell nuclear transfer (SCNT) embryo development. However, the mechanisms by which the DNA methylation affects the epigenetic reprogramming have not been fully elucidated. ***Methods:*** In our study, we used quantitative polymerase chain reaction (qPCR), Western blotting, immunofluorescence staining (IF) and sodium bisulfite genomic sequencing to examine the effects of RG108, a DNA methyltransferase inhibitor (DNMTi), on the dynamic pattern of DNA methylation and histone modifications in porcine SCNT embryos and investigate the mechanism by which the epigenome status of donor cells' affects SCNT embryos development and the crosstalk between epigenetic signals. ***Results:*** Our results showed that active DNA demethylation was enhanced by the significantly improving expression levels of *TET1*, *TET2*, *TET3* and 5hmC, and passive DNA demethylation was promoted by the remarkably inhibitory expression levels of *DNMT1*, *DNMT3A* and 5mC in embryos constructed from the fetal fibroblasts (FFs) treated with RG108 (RG-SCNT embryos) compared to the levels in embryos from control FFs (FF-SCNT embryos). The signal intensity of histone H3 lysine 4 trimethylation (H3K4me3) and histone H3 lysine 9 acetylation (H3K9Ac) was significantly increased and the expression levels of H3K4 methyltransferases were more than 2-fold higher expression in RG-SCNT embryos. RG-SCNT embryos had significantly higher cleavage and blastocyst rates (69.3±1.4%, and 24.72±2.3%, respectively) than FF-SCNT embryos (60.1±2.4% and 18.38±1.9%, respectively). ***Conclusion:*** Dynamic changes in DNA methylation caused by RG108 result in dynamic alterations in the patterns of H3K4me3, H3K9Ac and histone H3 lysine 9 trimethylation (H3K9me3), which leads to the activation of embryonic genome and epigenetic modification enzymes associated with

Ziyi Li
First Hospital, Jilin University
Changchun, Jilin130021 (China)
Tel. 86-431-8783-6187, E-Mail ziyi@jlu.edu.cn

H3K4 methylation, and contributes to reconstructing normal epigenetic modifications and improving the developmental efficiency of porcine SCNT embryos.

Introduction

Pigs are important livestock in agriculture and valuable animal models in therapeutic and basic biological research such as bioreactor, xenotransplantation and somatic cell nuclear transfer (SCNT). During SCNT, aberrant reprogramming of epigenetic modifications from the donor cell genome hampers extensive application of this procedure [1, 2]. Donor cell nuclei possess specific epigenetic information, which is encoded as DNA methylation and histone modifications [3]. DNA methylation and histone modifications are important epigenetic modifications involved in the regulation of gene expression, inheritance of chromatin states and genome stability [4, 5]. It is generally believed that developmental abnormalities are caused mainly by aberrant reprogramming of DNA methylation and histone modifications [6, 7].

Genome-scale DNA methylation studies revealed a connection between DNA methylation and histone modifications [8]. During epigenetic reprogramming of SCNT embryos, the DNA methylation dynamics can reflect epigenetic reprogramming in a way, therefore, the mechanism of epigenetic reprogramming in cloned embryos have focuses mainly on DNA demethylation and remethylation [7]. DNA methylation of early nuclear transfer (NT) embryos was found to be reprogrammed, generating an abnormal state, and the altered methylation status favoured the successful completion of the apparent reprogramming of SCNT embryos and promoted the normal development of the embryos [9]. DNA methylation reprogramming in early embryos is regulated by DNA methylation related genes.

To our knowledge, the effects of RG108, a DNMTi, on the dynamic pattern of DNMTs and histone modifications during the development of porcine preimplantation embryos are not fully elucidated. To facilitate nuclear reprogramming and thus improve cloning efficiency, some epigenetic modification chemicals, including DNMTi that decrease methylation levels, have been used [10, 11]. RG108, was found to be free of cytotoxic or genotoxic effects compared to other DNMTis, such as 5-aza-2-deoxycytidine (5-aza-dC) [12], zebularine [13], and epigallocatechin-3-gallate [14], and had been used to assist the somatic nucleus to mimic DNA methylation and chromatin remodeling. In pigs, RG108 treatment improved the developmental capacity of cloned embryos [15]. However, research into these potential applications progresses slowly in pigs, because the cloning efficiency is extremely low and no authentic porcine embryonic stem cells are currently available [16-19].

In this study, the fetal fibroblasts were treated with RG108 (RG108-FFs) and used as donor cells to construct SCNT embryos, to investigate the mechanism by which the donor cells' epigenome status affects SCNT embryos development and the crosstalk between epigenetic signals. This work revealed that changing the DNA methylation status of donor cells via the DNA methylation modification agents RG108 may be an effective way to improve the cloning efficiency and embryonic development of SCNT embryos.

Materials and Methods

Chemicals and animals

All chemicals and reagents were purchased from Sigma-Aldrich (St. Louis, MO, USA), unless otherwise noted. All animal treatments were conducted in accordance with the experimental procedures and standards approved by the Animal Welfare Research Ethics Committee of Jilin University. (Approval ID:20151008-1). RG108 was purchased from Selleck Chemicals (Houston, TX, USA).

Isolation and cultivation of fetal fibroblasts (FFs)

FFs were isolated from 30- to 35-day-old fetal pigs (approximately 35 mm in length). The fetus and all complete fetal membranes were placed in 75% ethanol for 5 minutes and then rinsed at least three times with phosphate-buffered saline (PBS). The fetus was carefully taken out from the fetal membranes, and the head, limbs and internal organs were removed and the remaining tissues were washed with PBS. Then, the remaining tissue were minced into fragments less than 1 mm^3 in a Petri dish. Five volumes of tissues of 0.25% trypsin were added to the tissue, and incubated at 37 °C, mixing every 5 min for a total of 20 min. An equal volume of Dulbecco's Modified Eagle's Medium (DMEM) (Gibco, MA, USA) supplemented with 10% fetal bovine serum (Gibco, MA, USA) and 0.1% penicillin/ streptomycin (v/v) (hereafter, "complete DMEM") was added to terminate the digestion, and then the cells were pelleted by centrifugation at 1000 rpm for 5 min. The cell pellet was suspended in complete DMEM medium, and then transferred to a culture dish (8-10 ml per dish). We attempted to ensure that each fetus was plated in one 100 mm dish, and the cells were incubated at 37 °C in 5% CO_2 until approximately 90% confluent, at which point they were passaged and frozen.

Collection and in vitro maturation of porcine oocytes

Porcine ovaries were collected from a local abattoir and transported to the laboratory at 35-38.5 °C within 2-4 h in 0.9% NaCl supplemented with penicillin. Cumulus oocyte complexes (COCs) were aspirated from 3- to 6- mm ovarian follicles using a 20-gauge needle attached to a 10 ml syringe. COCs with at least three layer of cumulus cells were selected and cultured in *in vitro* maturation (IVM) medium after washing twice with the PBS supplemented with 10% fetal bovine serum. Fifteen COCs were cultured in a 100 μl drop of maturation medium (TCM-199 supplemented with 26 mM sodium bicarbonate, 3.05 mM glucose, 0.91 mM sodium pyruvate, 10 μg/ml epidermal growth factor, 50 μg/ml luteinizing hormone, 50 μg/ml follicle-stimulating hormone, 0.1% polyvinyl alcohol [PVA] [w/v], 0.03% bovine serum albumin [BSA] [w/v], and 0.1% penicillin/streptomycin (Gibco, MA, USA)) for 22-24 h at 38.5 °C, 5% CO_2, and then changed to the same medium without hormone until for 42-44 h. Oocytes that contained the first polar body were considered mature.

In vitro fertilization (IVF)

Fresh porcine semen was purchased from the Jilin University pig farm and washed three times with Dulbecco's PBS containing 0.1% BSA(w/v), and centrifuged at 1000 rpm for 5 minutes. The sperms were resuspended in modified Tris-buffered medium (mTBM) containing 2 mg/ml BSA and 2 mM caffeine, and cultured for 30 min in the CO_2 Cell Culture Shelves (Thermo Scientific, Waltham, USA). Groups of 25 oocytes were transferred to 100 μl of the fertilization medium covered with paraffin oil. Fifty microliters of diluted sperms were added to 100 μl of the fertilization medium containing the oocytes. Yielding a final sperm concentration of $1.6–5.0×10^5$ sperm/ml. The oocytes were co-cultured with sperms for 6 hours at 38.5 °C with 5% CO_2, and then the oocytes were transferred to porcine zygote medium 3 (PZM3) for continued culture.

Table 1. Antibodies used for Immunofluorescence staining

Antibodies	RRIDs	Catalog No.	Manufacturer	Sources	Dilution ratio
5mC	RRID: AB-2687950	39649	Active Motif	Mouse	1:200
5hmC	RRID: AB-10013602	39769	Active Motif	Rabbit	1:200
H3K9Ac	RRID: AB-297491	ab10812	abcam	Rabbit	1:500
H3K9me3	RRID: AB-306848	ab8898	abcam	Rabbit	1:500
H3K4me3	RRID: AB-306649	ab8580	abcam	Rabbit	1:500
DNMT1	RRID: AB-731983	ab19905	abcam	Rabbit	1:500
β-actin	RRID: AB-306371	ab8226	abcam	Mouse	1:1000

Somatic cell nuclear transfer

The first polar body of matured oocytes was removed under an inverted microscope and using the blind-suction method. Approximately 10% of the cytoplasm, likely including the nucleus, was collected in drops of 5 μg/mL cytochalasin B. A donor cell was subsequently injected into the perivitelline space of the oocytes. The reconstructed embryos were cultured for 1 h in PZM3 and then activated by two successive direct-current pulses at 1.2 kV/cm for 30 μsec using an ECM2001 electro-fusion instrument (ECM2001, BTX, USA). The activated cloned embryos were then cultured in PZM3 medium at 38.5 ˚C with 5% CO_2 and 100% humidity for 7 days.

Western blotting

Protein samples were separated by Biofuraw™ Precast Gel (Tanon, shanghai, China), transferred to Immobilon-p transfer membrane (Millipore, MA, USA) and blocked with 5% nonfat milk/PBS. Membrane was incubated overnight at 4 °C with primary antibodies (Table 1). Membrane was washed 3 times with PBST and incubated for 1 h at room temperature (RT) with a horseradish peroxidase (HRP)-conjugated goat anti-rabbit (Proteintech, SA00001-2, 1:2000 dilution) or HRP-conjugated goat anti-mouse (Proteintech, SA00001-1, 1:2000 dilution) secondary antibody. Membrane was washed 3 times with PBST and visualized by Tanon 5200 Automatic fluorescence/chemiluminescence imaging analysis system (Tanon, shanghai, China). Densitometry analysis of Western blotting was performed using the ImageJ software (Rasband, WS, ImageJ, U. S. National Institutes of Health, Bethesda, Maryland, USA, http://imagej.nih.gov/ij/, 1997–2014).

Immunofluorescence (IF) staining

The zona pellucida of the embryos were digested using 0.5% pronase in PBS. After three washes with PBS-PVA, the zona pellucida-free embryos and FFs were fixed for 30 min at RT with 4% paraformaldehyde in PBS, permeabilized for 30 min with 0.2% Triton X-100 prepared in PBS, and then blocked for 1 h at 37 °C with 1% BSA (w/v) in PBS. The embryos and FFs were incubated overnight at 4 °C with primary antibodies (Table 1) and then embryos and FFs were washed with PBS-PVA and stained at 37 °C for 2 h with Alexa Fluor 488 goat anti-mouse (1:500 dilutions, A-11001) (Invitrogen, MA, USA) or Alexa Fluor 594 goat anti-rabbit (1:500 dilutions, A-11037) (Invitrogen, MA, USA) antibodies. The DNA was stained for 10 min with 10 μg/mL 4',6-diamidino-2-phenylindole (DAPI) prior to mounting and observation under a fluorescence microscope (Nikon, Tokyo, Japan).

Microscopy and image analysis

Fluorescence was examined with a Nikon Eclipse Ti-U microscope equipped with appropriate filters (Nikon, Tokyo, Japan). Images were captured using a DS-Ri2 CCD camera (Nikon, Tokyo, Japan) driven by NIS-Elements BR (Nikon, Tokyo, Japan) running on a Power PC Intel® Core™ i5-7400 computer (DELL, Texas, USA). Separate images for DAPI and Alexa Fluor 488/594 were captured digitally from double stained embryos and separated into their single-colour components.

Images were captured using the same microscope settings and exposure times. Evaluation of the total fluorescence intensity of individual images was performed using ImageJ software (National Institutes of Health, Bethesda, MD), based on procedures described elsewhere [20]. Background fluorescence intensity was measured as an average intensity level within the cytoplasmic area, and subtracted from the nuclear staining intensity for correction, and the labelling intensity of the nuclei of porcine embryos and donor cells was calculated accordingly. Semi-quantitative fluorescence intensity measurements were obtained by the labelling intensity of specific signal in each nucleus. Data shown are representative for at least three independent experiments.

RNA isolation and polymerase chain reaction (qPCR)

The REPLI-g® WTA single cell kit (Qiagen, Hilden, Germany) was used to extract the total RNA from the porcine embryos and synthesize cDNA. The primers used are listed in Table 2. Quantitative amplification of cDNA was performed in 96-well optical reaction plates using SYBR® Premix Ex TaqTM reagents (TaKaRa, Tokyo, Japan) and a Light Cycler® 96 Real-Time PCR System (Roche, Basel, Switzerland). Th–e qPCR mix (20 μl) included 10 μl of SYBR green premix, 1 μl of each forward and reverse primer (10 μM), 1 μl of cDNA and 7 μl of dH2O. The qPCR conditions were as follows: 30 s denaturation at 95 °C, 40 cycles of PCR for the quantitative analysis (95 °C for 5 s and 60 °C for 30 s), one cycle for the melting curve analysis (95 °C for 5 s,

60 °C for 1 min, 95 °C for 1 s) and cooling at 4 °C. The relative expression level for each gene was calculated using the $2^{-\Delta\Delta CT}$ method [21, 22]. The qPCR analysis was performed three times for each sample. Additionally, we defined the gene expression cut-off as a mean Ct value of 35. GAPDH was used as the reference gene.

Sodium bisulfite genomic sequencing

Genomic DNA was subjected to bisulfite transformation, followed by PCR using the primers listed in Table 3. The PCR products were gel recovered using an ordinary Axy Prep DNA Gel Extraction Kit (Axygen, Beijing, China) and then ligated into the T-Vector pMD19 (TaKaRa, Tokyo, Japan). Recombinant plasmids were transformed into DH5α competent cells (Tiangen, Beijing, China) and 20 positive clones were selected and sequenced (Sangon Biotech, Changchun, China).

Blastocyst apoptosis assays

Day-7 blastocysts were collected, the zona pellucida was removed by treatment with 0.5% pronase, and embryos were fixed for 30 min in 4% paraformaldehyde in PBS. Fixed blastocysts were permeabilized for 30 min at RT using 0.2% Triton X-100 in PBS, washed three times with PBS-PVA and incubated at 37 °C in the dark for 1 hour with terminal deoxynucleotidyl transferase dUTP nick end labelling (TUNEL) solution from the In Situ Cell Death Detection Kit (Roche, Mannheim, Germany). The embryos were washed three times with PBS-PVA, and incubated for 10 min with 10 μg/ml DAPI to stain the nuclei. The stained embryos were mounted between a cover slip and a glass slide, and examined under a fluorescence microscope.

Table 2. Primers used in the qPCR analysis

Gene	Gene ID	Primer sequences (5'-3')	Annealing temperature (°C)	Product size (bp)
BCL2	XR_002346028.1	F: CTTACCGAATGACCACCTAGAGC	60	182
		R: CCGACTGAAGAGCGAACCC		
BAX	XM_013998624.2	F: CGGGACACGGAGGAGGTTT	60	189
		R: CGAGTCGTATCGTCGGTTG		
POU5F1	NM_001113060.1	F: GTCGCCAGAAGGGCAAAC	57	125
		R: CAGGGTGGTGAAGTGAGGG		
NANOG	EF522119.1	F: CCCCGAAGCATCCATTTCC	58	101
		R: CGAGGGTCTCAGCAGATGACAT		
SOX2	NM_001278769.1	F: CCCTGCAGTACAACTCCATGAC	59	86
		R: GGTGCCCTGCTGCGAGTA		
CDX2	NM_001123197.1	F: AGTCGCTACATCACCATTCGGAG	59	116
		R: GCTGCTGTTGCTGCAACTTCTTC		
DNMT1	NM_001032355.1	F: GGCAGACCACCATCACATC	55	165
		R: GGAGCAGTCCGGCAACT		
DNMT3A	NM_001097437.1	F: GGACAAGAATGCCACCAAATCA	60	196
		R: CTTGCCGTCTCCGAACCA		
DNMT3B	NM_001348900.1	F: GGGTGGAAAGACACGGGAT	60	243
		R: TAGGAGCGTAGAAGCAAGGAA		
TET1	NM_001315772.1	F: TGTCGGCTTGGCAAGAAAGA	60	115
		R: AGACCACTGTGCTGCCATTA		
TET2	XM_013978993.2	F: GTGAGATCACTCACCCATCGCATA	60	123
		R: TACTGGCACTATCAGCATCACAGG		
TET3	XM_021087365.1	F: TCTTCCGTCGTTCAGCTACTACAG	60	127
		R: GTGGAGGTCTGGCTTCTTCTCAAA		
GAPDH	NM_001206359.1	F: CAAATTCATTGTCGTACCAG	60	90
		R: ACACTCACTCTTCTACCTTTG		

Table 3. Primers used in the bisulfite sequencing

GenBank ID	Name	Target	Primer Seq(5'-3')	CPG sites	Length
GU433187.1	NANOG	16	GGAGATTTAAAGGAGTTTTAGGTTAAGAAATCTCCTCCAAATATTAAAAATATCAAAAA	10	500bp
CT737281.12	POU5F1	515	GGGAGGTTTTTGGAAGTTTAGTTAGACAATCCCCTTAAAAAACCCTAAT	14	187bp
Z75640	CENREP	135859	GGTATTGTTGTTTGTTTGGTGATTAAAATTTATTCCTCAAACCCAATTT	11	231bp
AY044827.	H19 DMR1	136045	Outer F: AGGAGATTAGGTTTAGGGGAAT R: CTACCACTCCCCTCATACCTAA Inner F: AGTGTTTGGGGATTTTTTTTTT R: CACCCCATCCCCTAAATAACCCTC	48	
X56094.1	IGF2 DMR1	282	Outer F: GGAAGTTTTGTTTAGTTGGTTTTT [49] R: AAATCTAAAAACAAAAACAAAAAAC Inner F: GTTAGGTTTAGTGTTTAGTATTGGT R: TCCAAAACCAAACCTCTCCTAC	49	

RT^2 Profiler PCR Array and differential expression profiling

The Pig Epigenetic Chromatin Modification Enzymes RT^2 Profiler PCR Array (Qiagen, PASS-085Z) was performed according to the manufacturer's instructions. The detected genes are listed in Table 4. Gene expression was normalized using a panel of housekeeping genes including beta actin (*β-ACTIN*), beta-2 microglobulin (*B2M*), glyceraldehyde 3-phosphate dehydrogenase (*GAPDH*), hypoxanthine phosphoribosyl transferase 1 (*HPRT1*) and ribosomal protein L13a (*RPL13A*). Quality control was confirmed using a Gene Globe Data Analysis Center (Qiagen, Hilden, Germany). Only results that passed quality checks in PCR array reproducibility and genomic DNA contamination were included. Genes were required to show at least 2-fold differential expression, with P <0.05 between the experimental groups and the control groups to be considered significant for the purpose of this study.

Degust (http://vicbioinformatics.com/degust/), an interactive web tool for visualizing differential gene expression data, was used to generate the parallel coordinate plot (PCP) based on the data from the PCR array [23]. The relative expression values of each tested gene were provided as a ΔΔCT value to evaluate the transcript level. The significantly differential expression genes were assessed using the LIMMA package integrated in the Degust public server. Heat maps showing the genic relationship matrices were created in R studio Version 1.1.383 with the Heat map package [24]. The complete linkage hierarchical clustering was performed by the Euclidean distance measure.

Statistical analysis

All experiments were repeated at least three times. The statistical analysis was carried out by two-tailed Student's *t*-test using Statistics Production for Service Solution (SPSS) v19.0 software (Chicago, IL, USA). *P*-value <0.05 was considered statistically significant, and P <0.01 was considered extremely significant.

Table 4. Gene table for RT^2 Profiler PCR Array

GenBank	Symbol	Description
XM_003125708	ASH1L	Probable histone-lysine N-methyltransferase ASH1L-like
NM_001243568	ASH2L	Ash2 (absent, small, orhomeotic)-like (Drosophila)
XM_003133491	ATF2	Activating transcription factor 2
NM_001025225	AURKA	Aurora kinase A
NM_213919	AURKB	Aurora kinase B
XM_003354497	BAZ1B	Bromodomain adjacent to zinc finger domain, 1B
XM_003123208	CARM1	Coactivator-associated arginine methyltransferase 1
XM_001927509	CDYL	Chromodomain protein, Y-like
XM_005662139	CIITA	Class II, major histocompatibilitycomplex,
XM_001924382	CSRP2BP	CSRP2 binding protein
XM_003121437	CXXC1	CXXC finger protein 1
NM_001032355	DNMT1	DNA (cytosine-5-)-methyltransferase 1
NM_001097437	DNMT3A	DNA (cytosine-5-)-methyltransferase 3 alpha
XM_001928593	DNMT3B	DNA (cytosine-5-)-methyltransferase 3 beta
XM_005674632	DOT1L	DOT1-like histone H3K79 methyltransferase
XM_005670237	DZIP3	DAZ interacting protein 3,zinc
NM_001101823	EHMT2	Euchromatic histone-lysine N-methyltransferase 2
XM_001929213	EP300	E1A binding protein p300
XM_003130718	EPC1	Enhancer of polycomb homolog1-like
XM_003127852	ESCO1	Establishment of cohesion 1homolog
XM_003483396	ESCO2	Establishment of sister chromatidcohesion
NM_001244309	EZH2	Enhancer of zeste homolog2
XM_003354838	FBXO11	F-box protein 11
XM_005671969	HAT1	Histone acetyltransferase 1
XM_003126776	HDAC10	Histone deacetylase 10-like
XM_005669815	HDAC11	Histone deacetylase 11
XM_001925318	HDAC2	Histone deacetylase 2
NM_001243827	HDAC3	Histone deacetylase 3
XM_005657593	HDAC4	Histone deacetylase 4
XM_003360315	HDAC6	Histone deacetylase 6
XM_005667668	HDAC9	Histone deacetylase 9
NM_001244268	ING3	Inhibitor of growth family,member
XM_003131405	KAT2A	K(lysine) acetyltransferase 2A
XM_003358330	KAT2B	K(lysine) acetyltransferase 2B
NM_001243915	KAT5	K(lysine) acetyltransferase 5
XM_005674537	KAT6A	K(lysine) acetyltransferase 6A
XM_001928949	KAT6B	K(lysine) acetyltransferase 6B
XM_003124470	KAT8	K(lysine) acetyltransferase 8
NM_001112687	KDM1A	Lysine (K)-specific demethylase 1A
XM_005668019	KDM5B	Lysine (K)-specific demethylase 5B
NM_001097433	KDM5C	Lysine (K)-specific demethylase 5C
XM_005657029	KDM6B	Lysine (K)-specific demethylase 6B
XM_003357320	KMT2A	Myeloid/lymphoid or mixed-lineage leukemia(trithorax
XM_005654261	KMT2C	Lysine (K)-specific methyltransferase 2C
XM_005667720	KMT2E	Lysine (K)-specific methyltransferase 2E
XM_003126953	LOC100512284	SET domain containing 6
XM_003360365	LOC100523762	Histone deacetylase 8-like
XM_003355640	LOC100627559	Histone deacetylase 7-like
XM_005658916	LOC767626	Suppressor of variegation 3-9-likeprotein
XM_005674561	MBD2	Methyl-CpG binding domain protein2
XM_003126111	MLL2	Myeloid/lymphoid or mixed-lineage leukemia2
XM_003127968	MYSM1	Myb-like, SWIRM and MPNdomains
NM_001195359	MYST2	K(lysine) acetyltransferase 7
NM_001025228	NCOA1	Nuclear receptor coactivator 1
NM_001114276	NCOA3	Nuclear receptor coactivator 3
XM_003483942	NCOA6	Nuclear receptor coactivator 6
XM_003122163	NEK6	NIMA (never in mitosisgene
XM_003123667	NSD1	Nuclear receptor binding SETdomain
XM_005667164	PAK1	P21 protein (Cdc42/Rac)-activated kinase1
XM_003355999	PRMT1	Protein arginine methyltransferase 1
XM_005658906	PRMT2	Protein arginine methyltransferase 2
NM_001160093	PRMT5	Protein arginine methyltransferase 5
NM_001190183	PRMT6	Protein arginine methyltransferase 6
XM_003126909	PRMT7	Protein arginine N-methyltransferase 7-like
XM_003481700	PRMT8	Protein arginine methyltransferase 8
XM_003354538	RNF40	E3 ubiquitin-protein ligase BRE1B-like
XM_003484085	RPS6KA3	Ribosomal protein S6 kinase,90kDa,
XM_005655086	SETD1A	SET domain containing 1A
XM_005670628	SETD1B	SET domain containing 1B
XM_005669478	SETD2	SET domain containing 2
XM_001925288	SETD3	SET domain containing 3
XM_003358943	SETD4	SET domain containing 4
XM_001927800	SETD5	SET domain containing 5
XM_005656533	SETD7	SET domain containing (lysinemethyltransferase)
XM_005670605	SETD8	SET domain containing (lysinemethyltransferase)
XM_005663486	SETDB1	SET domain, bifurcated 1
XM_003130966	SETDB2	Calcium binding protein 39-like
NM_001160089	SMYD1	SET and MYND domaincontaining
NM_001160092	SMYD3	SET and MYND domaincontaining
XM_003122431	SUV420H1	Histone-lysine N-methyltransferase SUV420H1-like
XM_001927284	UBE2A	Ubiquitin-conjugating enzyme E2A
NM_001257356	UBE2B	Ubiquitin-conjugating enzyme E2B
XM_003358897	USP16	Ubiquitin carboxyl-terminal hydrolase 16-like
XM_003128809	WHSC1	Probable histone-lysine N-methyltransferase NSD2-like
XM_003357928	ACTB	Actin, beta
NM_213978	B2M	Beta-2-microglobulin
NM_001206359	GAPDH	Glyceraldehyde-3-phosphate dehydrogenase
NM_001032376	HPRT1	Hypoxanthine phosphoribosyltransferase 1
NM_001244068	RPL13A	Ribosomal protein L13a

Results

Effect of RG108 on development related-gene expression and the DNA methylation status in FFs

To screen the optimum concentration of RG108, the fibroblasts were treated with different concentrations of RG108 (0, 10, 20, 50, 75 and 100 μM) for 48h, and then fluorescent immunostaining of global DNA methylation was carried out by staining with 5mC (Fig. 1A,1B,1C,1D,1E and 1F). Western blotting (Fig. 1H) was performed to analyse the expression of DNMT1 in FFs. Our results showed that FFs treated with 10 μM and 20 μM RG108 had remarkably lower relative DNA methylation of 5mC than those in the other groups (Fig. 1G). The FFs treated with 20 μM, 50 μM and 100 μM RG108 showed significant lower expression of DNMT1 than those in the other groups (Fig. 1I). On the basis of the above results, we selected 20μM as the most appropriate concentration of RG108 and used that concentration for the following experiments.

Compared with FFs, RG108-FFs showed significantly up-regulated expression of pluripotency-related genes *NANOG, POU5F1, SOX2* and *CDX2* (Fig. 2A) and demethylation-related genes *TET1, TET2* and *TET3* (P<0.05) (Fig. 2D), whereas only the DNMT gene *DNMT1* (Fig. 2C) was remarkably down-regulated in expression (P<0.01). This global trend in DNA methylation was further evaluated at the promoter regions of *H19*, *IGF2*, *NANOG*

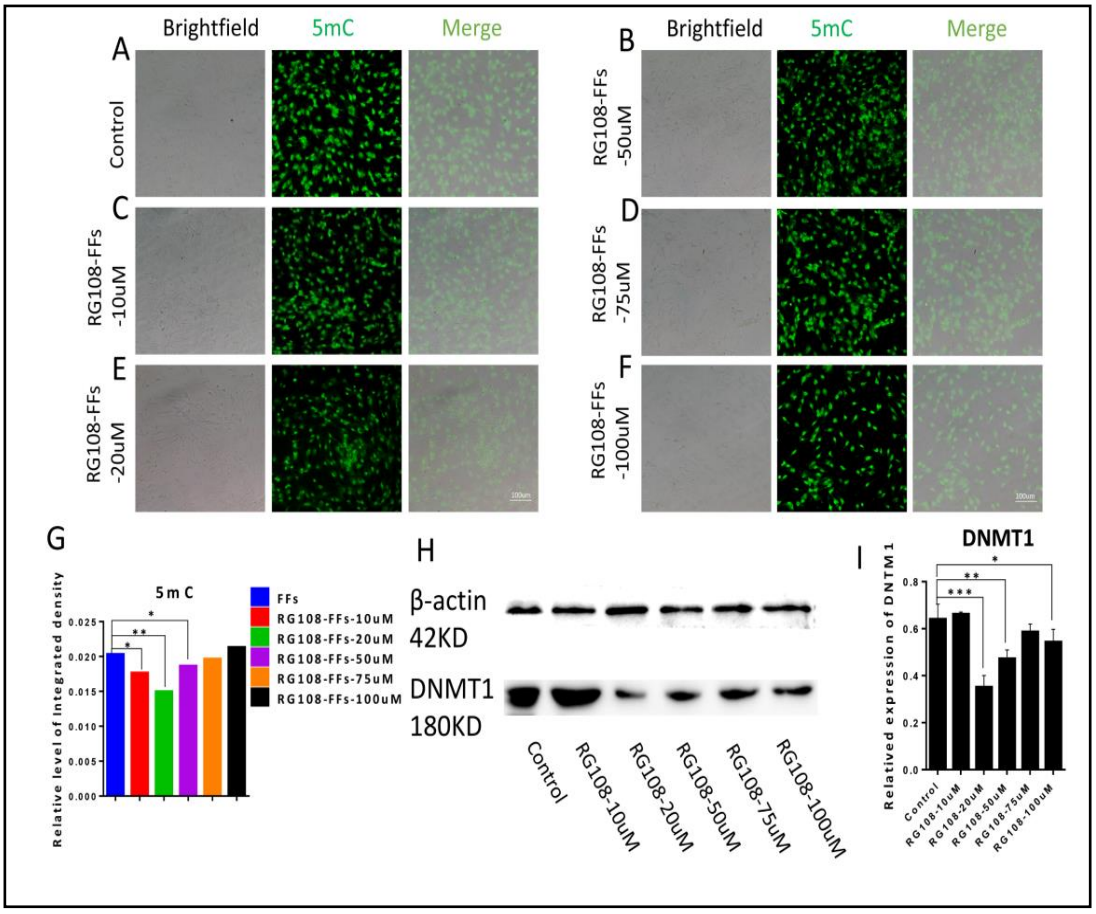

Fig. 1. Screening for the optimum concentration of RG108. Immunofluorescence staining of 5mC (green) in fetal fibroblasts at different concentrations of RG108 (0, 10, 20, 50, 75 and 100 ¦ÌM) (A, B, C, D, E and F). Scale bars, 100 ¦Ìm. (G) Semi-quantitative fluorescence intensity analysis of the 5mC staining. (H) Western blot analysis of DNMT1 in fetal fibroblasts at different concentrations of RG108 (0, 10, 20, 50, 75 and 100 ¦ÌM). (I) Quantitative gray analysis of DNMT1 in fetal fibroblasts at different concentrations of RG108.

and *Centromeric Repeat* (*CENREP*) using bisulfite-sequencing PCR (BSP) in RG108-FFs. The *NANOG* promoter region was hypomethylated in RG108-FFs (Fig. 2E, 3.6%). We chose the *H19*/*IGF2* locus as a representative for imprinted genes. The bisulfite sequencing on the DMR1 of *H19* and *IGF2* (Fig. 2F and 2G) gene locus showed moderate DNA methylation levels. DNA methylation in repeat elements is essential for maintaining chromosome stability [25]. The bisulfite sequencing of *CENREP* showed moderate DNA methylation levels (Fig. 2H, 48.5%) in RG108-FFs. Compared with the FFs, the DNA methylation levels of *NANOG* and *H19* remarkably decreased in RG108-FFs relative to control FFs, and there was no significant difference in *IGF2* and *CENREP* between the two groups (Fig. 2I, 2J, 2K and 2L).

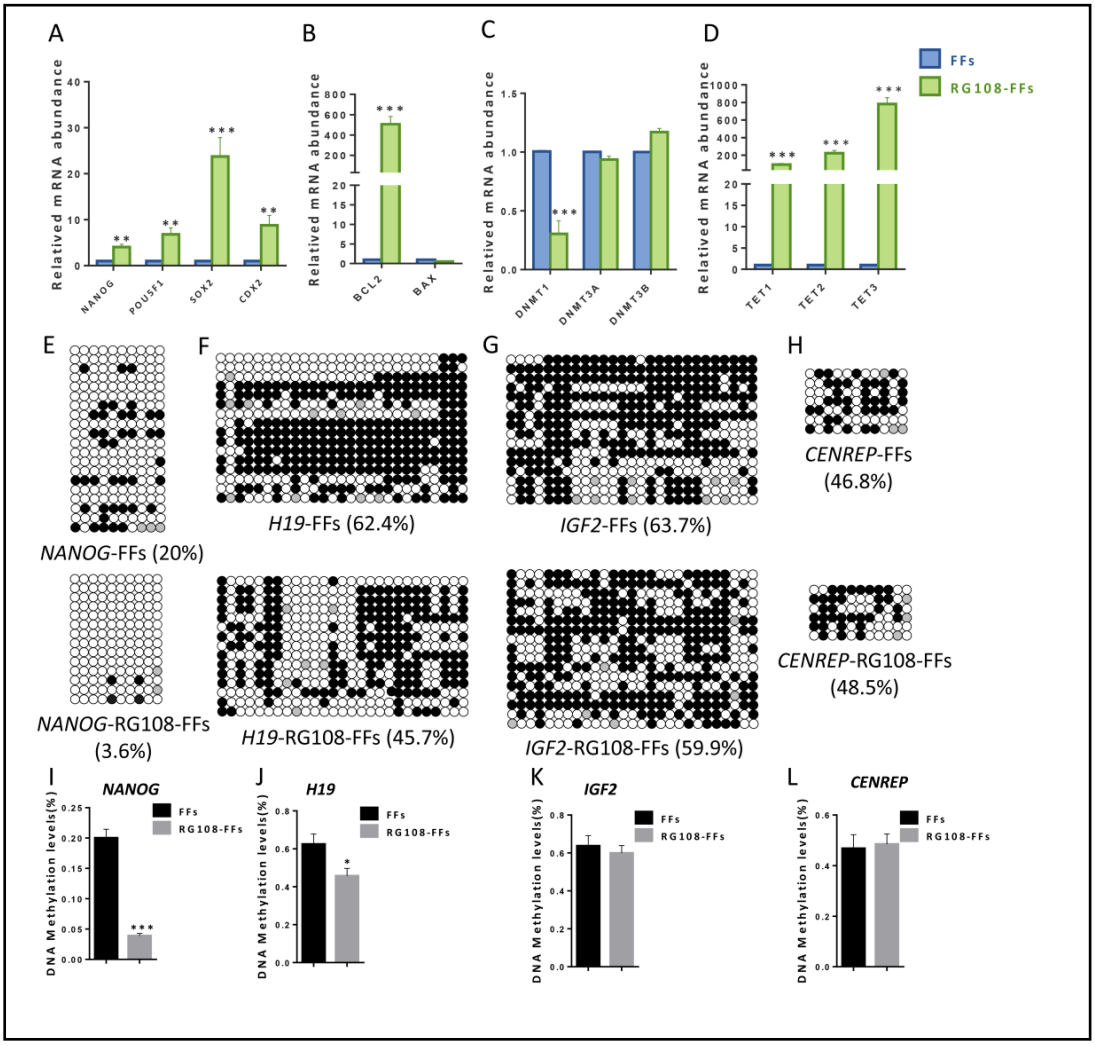

Fig. 2. Development related-gene expression and the DNA methylation situation in RG108-FFs. Relative abundance of the pluripotency genes (A), apoptosis-related genes (B), DNA methylation related genes (C) and demethylation-related genes (D) transcript in RG108-FFs and FFs. Quantities were normalized to GAPDH abundance. Transcript abundance in FFs was used to calibrate the samples (expression set to 1). DNA methylation in FFs and RG108-FFs, measured using bisulfite sequencing, at the promoter regions of NANOG (E, I), H19 (F, J), IGF2 (G, K), and CENREP (H, L). FFs, fetal fibroblast; CENREP, Centromeric Repeat. Data presented as the mean ¡À standard deviation. *, P< 0.05; **, P<0.01, as indicated.

RG108 improved the expression of epigenetic chromatin modification enzymes in FFs

To further study the effect of RG108 on the epigenetic interplay between DNA methylation and histone modifications, we performed a pig epigenetic chromatin modification enzymes RT^2 Profiler PCR Array in RG108-FFs and FFs. This PCR array can detect 84 representative genes encoding porcine epigenetic chromatin modification enzymes known or predicted to modify genomic DNA and histones to regulate chromatin accessibility and resulting genes expression, including DNA methylation/demethylation (3), histone acetylation/deacetylation (31), histone methylation (37), phosphorylation (16), and ubiquitination (9) as well as chromosome structural regulation. According to the analytical results, 14 enzymes had greater than 2-fold higher expression in the RG108-FFs than in the control FFs, and 15 enzymes with more than 2-fold lower expression in RG108-FFs. We classified the 14 over-expression enzymes and found that they were mainly transcriptional activation enzymes, including histone methyltransferases (H3K4 specific) (*ASH1L*, *CXXC1*, *SMYD3*, *LOC100512284 and LOC100523762*) and histone acetyltransferases (*EP300* and *KAT2A*) (Fig 3A). Meanwhile, we found that 15 downregulated enzymes were mainly related to transcriptional inhibition, which included histone methyltransferases (H3K9 and H3K27 specific) (*WHSC1*, *SETDB2*, and *SUV420H1*), DNMTs (*DNMT1*), histone deacetylases (*HDAC9* and *HDAC4*), and deubiquitinating enzymes (*LOC100511137* and USP16) (Fig. 3B).

We also detected several kinds of the most crucial epigenetic modification in RG108-FFs and FFs using IF microscopy. RG108-FFs had remarkably lower levels of repressive markers (DNMT1 and H3K9me3) (Fig. 3D, 3H, 3E and 3I), and significantly higher expression levels of active epigenetic markers (histone H3 modifications: H3K9Ac and H3K4me3) (Fig. 3F, 3J, 3G and 3K) than control FFs.

Treatment with RG108 improved the developmental capacity of SCNT embryos

The developmental capacity of IVF embryos or SCNT embryos constructed from donor RG108-FFs (RG-SCNT embryos) or FFs (FF-SCNT embryos) were evaluated. The results showed that the cleavage and blastocyst rates in the RG-SCNT embryos (69.30±1.21% and 24.72±2.3%, respectively) were significantly higher than those in the FF-SCNT embryos (60.1±0.83% and 18.38±1.9% respectively) (Table 5).

RG108 promoted the dynamic patterns of DNA methylation during early development in SCNT embryos

To further understand dynamic expression patterns of DNA methylation during early embryo development, we examined DNA methylation reprogramming related genes including DNMT-related genes (*DNMT1, DNMT3A* and *DNMT3B*) (Fig. 4A, 4B and 4C) and ten eleven translocation (*TET*) dioxygenases-related genes (*TET1, TET2* and *TET3*) (Fig. 4D, 4E and 4F) by qPCR methodology.

Compared with IVF embryos, the expression patterns of DNA methylation reprogramming related genes were disrupted in SCNT embryos. For DNA methylation related genes, cloned embryos showed significantly ($P < 0.05$) higher expression of *DNMT1* and *DNMT3B* from the 2-cell to blastocyst stages, and the same is true for the *DNMT3A* transcripts except for at the 2-cell stage, suggesting that DNA demethylation was incomplete in the cloned embryos. Additionally, there was significantly ($P < 0.05$) lower expression of *TET1*, *TET2* and *TET3* from the 4-cell to the blastocyst stage while *TET3* had a higher level of expression in the 2-cell stage, indicating that the active demethylation was not effectively activated before zygotic genome activation (ZGA).

When cloned embryos were reconstructed with RG108-FFs, compared with FF-SCNT embryos, had significantly ($P < 0.05$) lower expression levels of *DNMT1* and *DNMT3A* from the 2-cell to 4-cell stage and higher expression levels of *DNMT1*, *DNMT3A* and *DNMT3B* at the blastocyst stage. Meanwhile, compared to the FF-SCNT embryos, the RG-SCNT embryos had significantly ($P < 0.05$) higher transcripts of *TET3* from the 2-cell to the blastocyst stage, except during the 8-cell stage, and significantly ($P < 0.05$) lower transcripts of *TET1* and *TET2* in the 2-cell stage while higher expression of *TET1* and *TET2* in the blastocyst stage. In

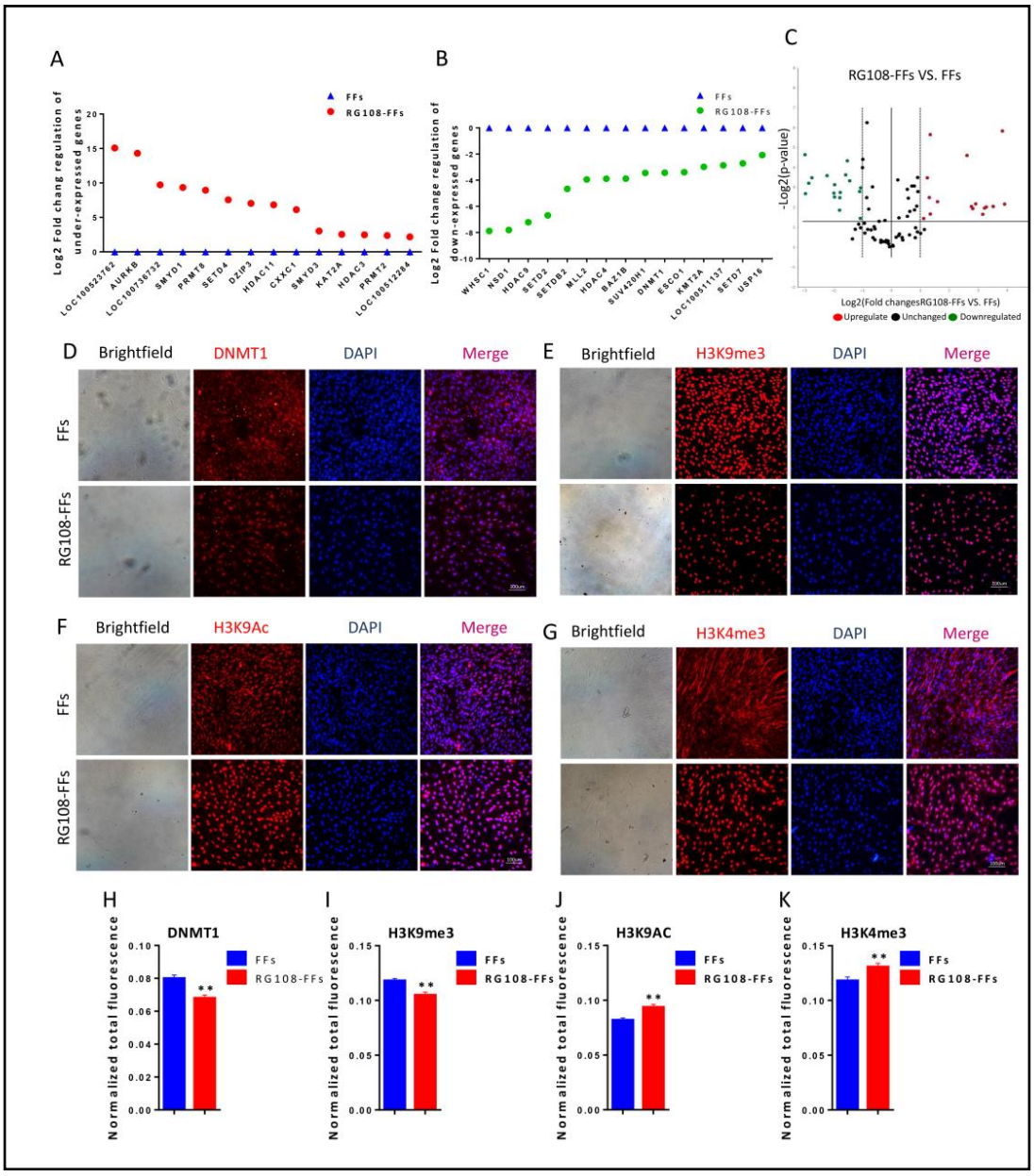

Fig. 3. RG108 improved the expression of epigenetic chromatin modification enzymes and histone modification in FFs. (A) differentially expressed genes (DEGs) of epigenetic chromatin modification enzymes were more than 2-fold higher expression in RG108-FFs. (B) DEGs of epigenetic chromatin modification enzymes were more than 2-fold lower expression in RG108-FFs. (C) Volcanic plot showed differentially expressed genes of epigenetic chromatin modification enzymes in RG108-FFs. (D-G) Immunofluorescence staining for DNMT1 (D), H3K9me3 (E), H3K9Ac (F) and H3K4me3 (G) in RG108-FFs. Nuclei are shown in blue. Scale bars, 100 ¦Ìm. (H-K) Semi-quantitative fluorescence intensity of DNMT1 (H) and histone markers (I-K) in RG108-FFs and FFs. Data presented as the mean ¡À standard deviation. *, P< 0.05; **, P<0.01.

comparison *with* IVF embryos, RG-SCNT embryos displayed significantly ($P < 0.05$) higher transcripts of *DNMT*1 and *DNTM3A* from the 4cell to the blastocyst stage, and *DNTM3B* at the 2-cell and blastocyst stage, although there was significantly ($P < 0.05$) lower transcripts of *TET1* and *TET2* from the 2-cell to the 8-cell stage and *TET3* had a remarkably higher expression level at the 2-cell and 4-cell stage. In addition, similar expression levels of *TET1*, *TET2* and *TET3* were detected at the blastocyst stage between IVF and RG-SCNT embryos.

Table 5. The treatment of RG108 improved the development capacity of SCNT embryos. Values in the same column with different superscripts (a, b and c) differ significantly (P < 0.05). Mean ± standard error is reported (n= 3 independent replicates). FFs: fetal fibroblasts, IVF: *In Vitro* Fertilization

Donor cell	No. of embryos	No. of embryos cleaved（%±SE）	No.of blastocysts （%±SE）	Total cell no. per blastocyst
FFs	210	126(60.1±2.4) [a]	34(18.38±1.9) [a]	39.33±0.88 [a]
RG108-FFs	223	154(69.3±1.4) [b]	44(24.72±2.3) [b]	47.67±2.45 [b]
IVF	182	125(68.7±2.2) [b]	44(30.1±3.3) [C]	55.12±3.41[C]

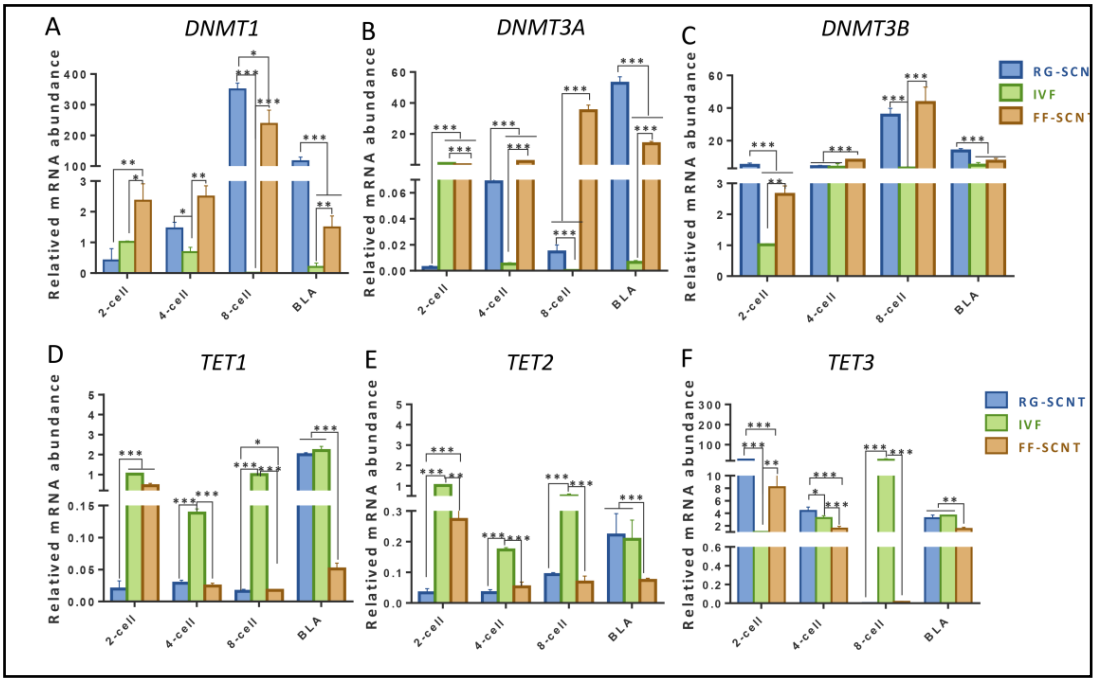

Fig. 4. The dynamic changes of DNMTs and TETs in the RG-SCNT, FF-SCNT and IVF embryos during early development. Relative abundance of the DNA methylation related genes DNMT1 (A), DNMT3A (B) and DNMT3B(C) or demethylation-related genes TET1(D), TET2(E) and TET3(F) transcript in porcine RG-SCNT, IVF and FF-SCNT embryos. Quantities were normalized to GAPDH abundance. Data presented as the mean ¡À standard deviation. *, P< 0.05; **, P<0.01 between groups, as indicated. BLA, blastocyst; RG-SCNT, RG108-FFs somatic cell nuclear transfer; FF-SCNT, somatic cell nuclear transfer.

Thus, the expression patterns of DNA methylation reprogramming related genes were improved in RG-SCNT embryos, which is beneficial for DNA methylation reprogramming.

IF staining for 5mC and 5hmC revealed that global DNA methylation in the FF-SCNT and RG-SCNT embryos. The overall 5hmC levels in FF-SCNT embryos were predominantly lower than that in IVF embryos. The RG-SCNT embryos had a significantly higher level of 5hmC than that in IVF and FF-SCNT embryos at the 2-cell and blastocyst stage, but more

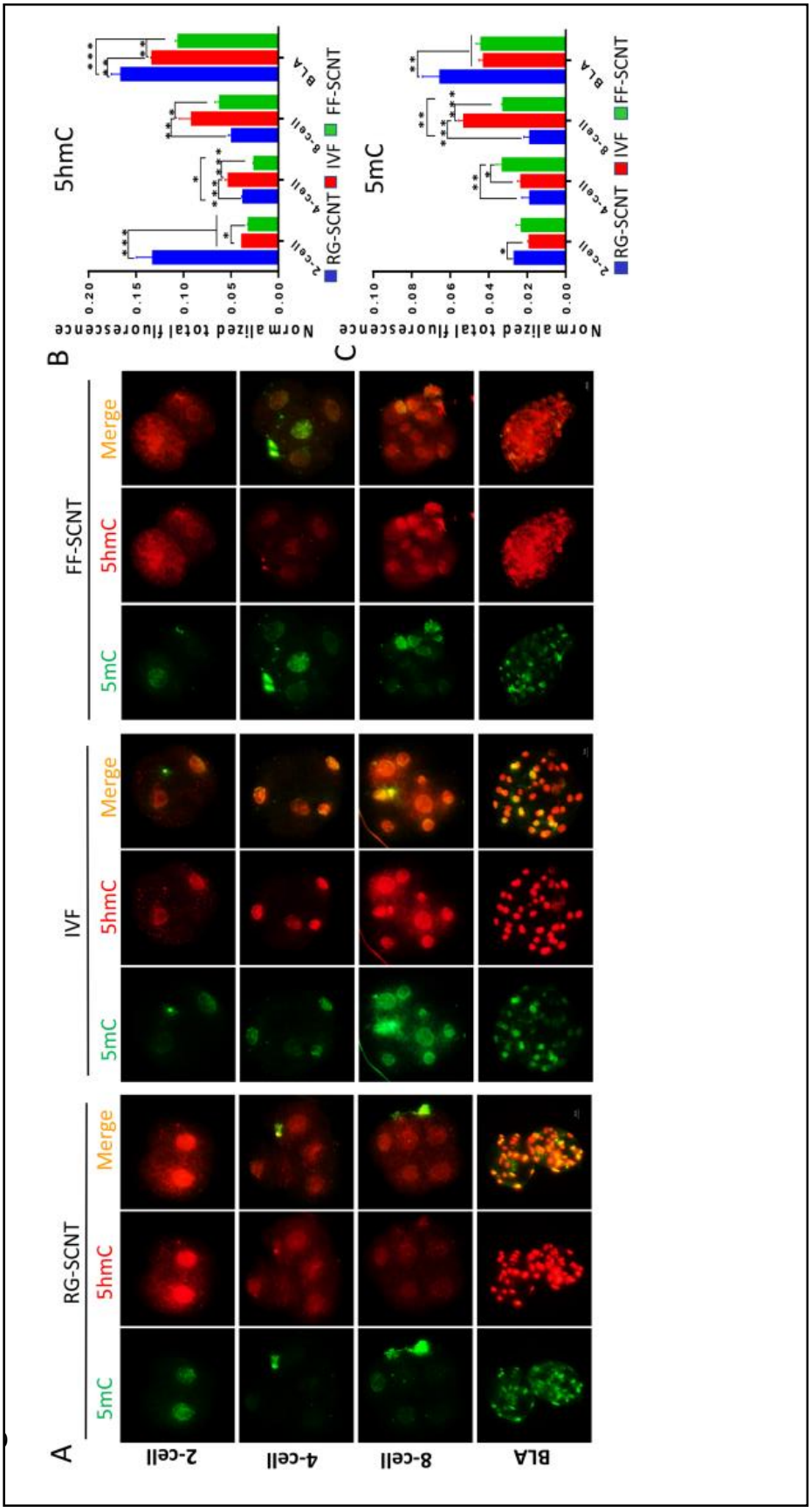

Fig. 5. Global DNA methylation in the SCNT and IVF embryos during early development. (A) Immunofluorescence staining of 5mC (green) and 5hmC (red) in RG-SCNT, IVF and FF-SCNT embryos. Scale bars, 25 ¦Ìm. (B-C) Semi-quantitative fluorescence intensity analysis of the 5mC (B) and 5hmC (C) staining. Data presented as the mean ¡À standard deviation. *, P< 0.05; **, P<0.01 between groups, as indicated. BLA, blastocyst; RG-SCNT, RG108-FFs somatic cell nuclear transfer; FF-SCNT, somatic cell nuclear transfer.

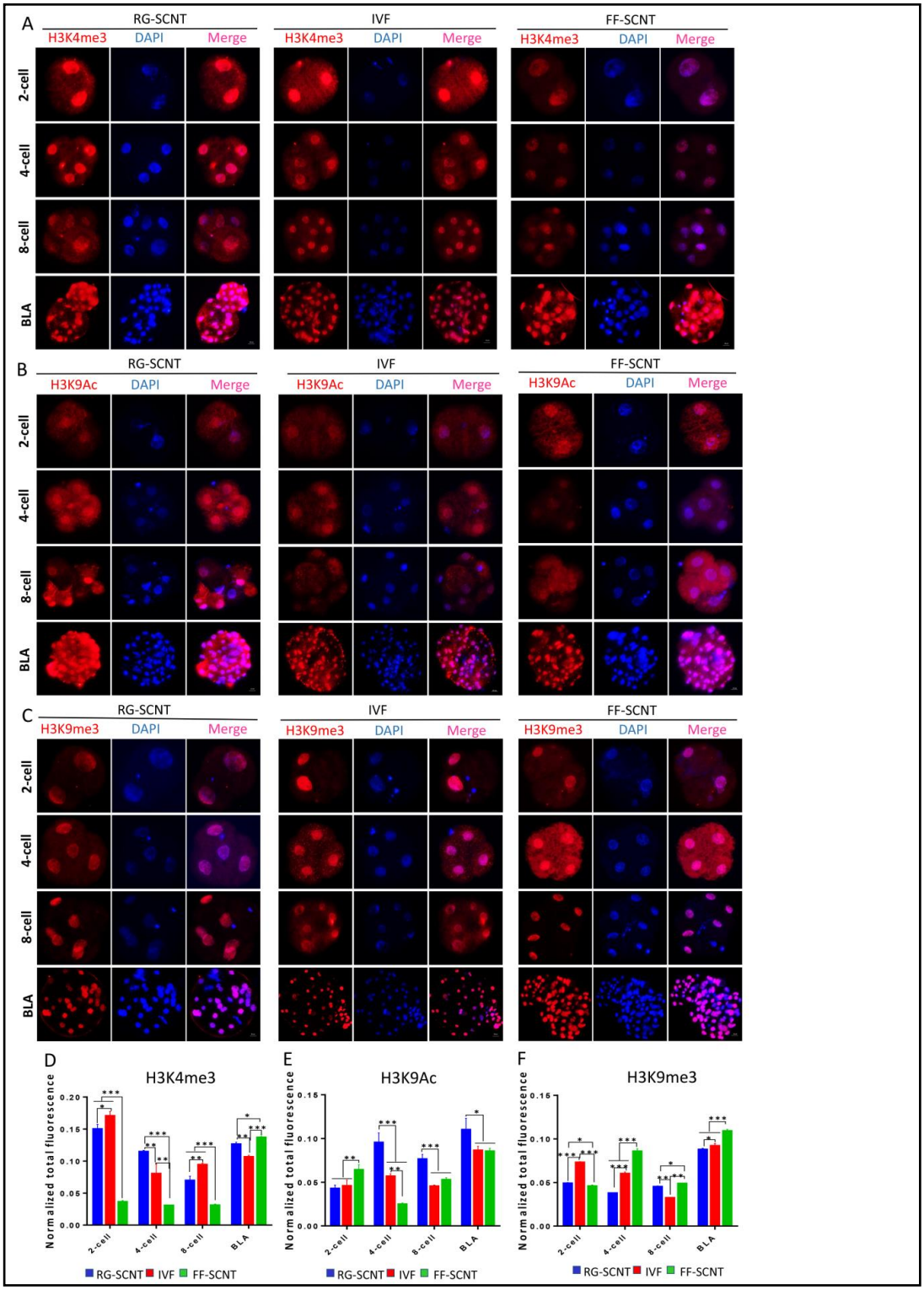

Fig. 6. The expression levels of H3K4me3, H3K9Ac and H3K9me3 in the SCNT and IVF embryos. (A-C) Immunofluorescence staining of H3K4me3 (A), H3K9Ac (B) and H3K9me3 (C) in the RG-SCNT, IVF and FF-SCNT embryos. Scale bars, 25 ¡Ìm. (D-F) Semi-quantitative fluorescence intensity analysis of the H3K4me3 (D), H3K9Ac (E) and H3K9me3 (F) staining. Data presented as the mean ¡À standard deviation. *, P< 0.05; **, P<0.01 between groups, as indicated. BLA, blastocyst; RG-SCNT, RG108-FFs somatic cell nuclear transfer; FF-SCNT, FFs somatic cell nuclear transfer.

similar to the IVF embryos than the FF-SCNT embryos (Fig. 5A). The 5hmC levels in FF-SCNT embryos were remarkably lower than that in the IVF and RG-SCNT embryos at the 2-cell, 4-cell and blastocyst stage (Fig. 5B). The RG-SCNT embryos had significantly lower levels of 5mC than that in the FF-SCNT embryos at the 4cell and 8cell stage, but higher levels at the blastocyst stage. Compared with IVF embryos, the 5mC levels in the RG-SCNT embryos were remarkable higher at the 2cell and blastocyst stage (Fig. 5C).

Effect of RG108 on the dynamic reprogramming of H3K4me3, H3K9Ac and H3K9me3 during the early development of SCNT embryos

The status of H3K4me3, H3K9Ac and H3K9me3 were assessed using IF microscopy (Fig. 6A, 6B and 6C). The results showed that each modification had its special dynamic change characteristic. The signal intensity of H3K4me3 in RG-SCNT embryos was significantly higher than that in its NT counterparts from the 2-cell to the 8-cell stage, but the intensity was lower at the blastocyst stage. In addition, the H3K4me3 levels in RG-SCNT embryos were remarkably higher than that in IVF embryos at the 4-cell and blastocyst stage (Fig. 6D). The levels of H3K9Ac in RG-SCNT embryos were significantly higher than that in the IVF and FF-SCNT embryos from the 4-cell stage to the blastocyst stage, especially during the 4-cell zygotic gene activation stage (Fig. 6E). The levels of H3K9me3 in RG-SCNT embryos were significantly lower than that in IVF and FF-SCNT embryos at the 4-cell and blastocyst stage (Fig. 6F). By detecting the dynamic changes of H3K4me3, H3K9Ac and H3K9me3 during the embryonic development, we found that the RG-SCNT embryos had dramatically improvements of abnormal histone modification, especially in the 4-cell zygotic gene activation stage.

RG108 treatment rescued the abnormal epigenetic reprogramming in the 4-cell SCNT embryos

We speculated whether abnormal ZGA might be caused by abnormal epigenetic modification in porcine SCNT embryos. Therefore, we next performed a study on the dynamic changes of DNA methylation and histone modification at the 4-cell stage. This trend in DNA methylation was further evaluated at the promoter regions of *POU5F1*, *NANOG*, and *CDX2* using BSP.

The global DNA methylation pattern at the promoter regions of *NANOG*, *POU5F1*, *CENREP*, *H19* and *IGF2* were analysed by BSP. The DNA methylation levels of *NANOG*, *POU5F1* and *CENREP* in the RG-SCNT embryos were lower than those in the FF-SCNT embryos but higher than in the IVF embryos (Fig. 7A, 7B and 7C). Meanwhile, we found that the DNA methylation levels of *H19* in the RG-SCNT embryos were higher than that in the FF-SCNT embryos but lower than in the IVF embryos and the *IGF2* levels in the RG-SCNT embryos were lower than in the FF-SCNT embryos but higher in the IVF embryos. (Fig. 7D and 7E).

Then, we performed a pig epigenetic chromatin modification enzymes RT^2 profiler PCR array in porcine IVF 4-cell (IVF-4C), FF-SCNT 4-cell (FF-SCNT-4C) and RG-SCNT 4-cell (RG-SCNT-4C) embryos. Using the IVF embryos as a positive control, the results showed that compared with the FF-SCNT embryos, some of the abnormal expression of chromatin modification enzymes were rescued in the RG-SCNT embryos (Fig. 8A and 8B). The cluster analysis showed that the expression pattern of 84 epigenetic chromatin modification enzymes in RG-SCNT embryos was closer to the IVF embryos (Fig. 8C). A volcanic plot showed that there were 19 genes up-regulated by at least 2-fold in the IVF and RG-SCNT embryos compared with that in the FF-SCNT embryos. All 19 genes had P-values <0.05 or smaller (Fig. 8D and 8E). We classified the 19 over-expressed enzymes and found that they were mainly transcriptional activation enzymes, including histone methyltransferases (H3K4 specific) (*ASH2L*, *ASH1L*, *MLL2*, *SETD1A* and *KMT2C*), histone acetyltransferases (*KAT2A*, *KAT6B* and *KAT8*), ubiquitin conjugating enzyme (*UBE2B* and *RNF40*), Nuclear Receptor Coactivator (*NCOA3* and *NCOA6*) and serine/threonine kinases, *PRS6KA3*. Nine genes were down-regulated by at least 2-fold in IVF and RG-SCNT embryos compared with that in FF-SCNT embryos; these genes included transcriptional inhibition enzymes (*USP16*,

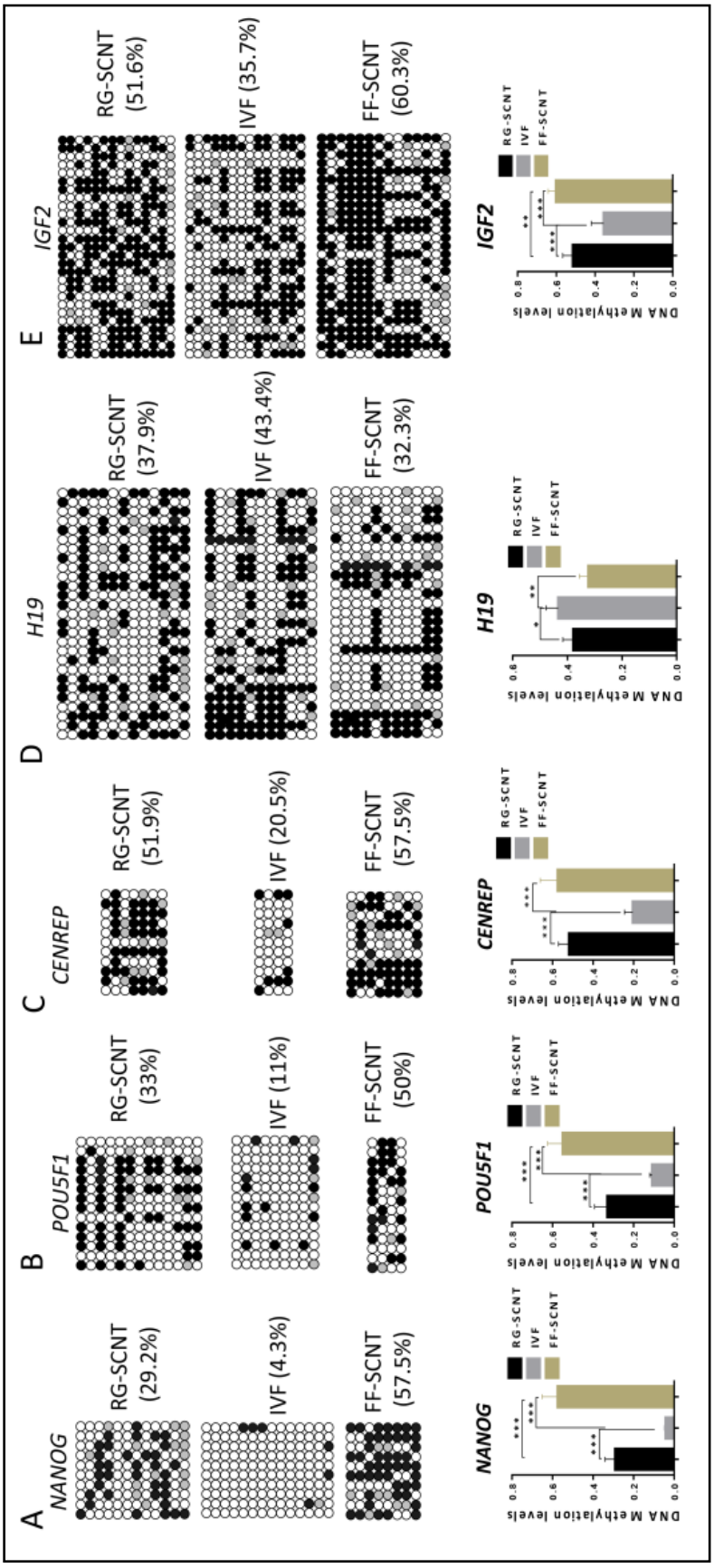

Fig. 7. RG108 treatment rescued the abnormal epigenetic reprogramming in the 4-cell SCNT embryos. (A-E) DNA methylation of the SCNT and IVF embryos at the 4-cell stage. DNA methylation in the RG-SCNT, IVF and FF-SCNT embryos, measured using bisulfite sequencing, at the promoter regions of NANOG (A), POU5F1 (B), CENREP (C), H19 (D), and IGF2 (E). CENREP, Centromeric Repeat; RG-SCNT, RG108-FFs somatic cell nuclear transfer; FF-SCNT, FFs somatic cell nuclear transfer. Data presented as the mean ¡À standard deviation. *, P <0.05; **, P <0.01, as indicated.

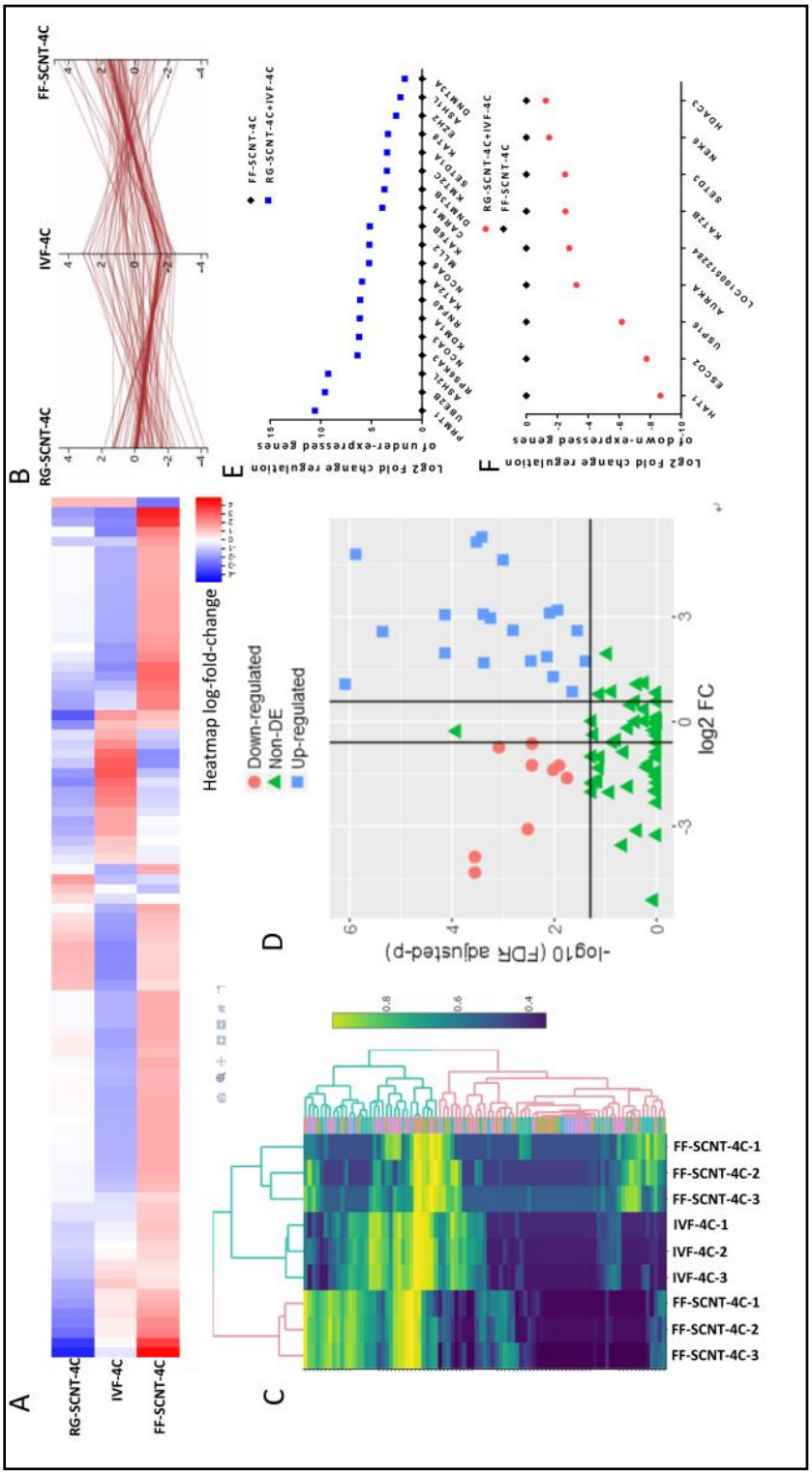

Fig. 8. RG108 treatment rescued the abnormal epigenetic reprogramming in the 4-cell SCNT embryos. (A and B) Parallel coordinate plots and heat map illustration of DEGs of epigenetic chromatin modification enzymes at the 4cell stage derived from RG-SCNT, IVF and FF-SCNT embryos. Absolute (abs) value of log fold change (FC) value >1, false discovery rate (FDR) cut-off value <0.05. (C) The cluster analysis of the 84 epigenetic chromatin modification enzymes expression pattern in RG-SCNT, IVF and FF-SCNT embryos at the 4cell stage. (D) Volcanic plot showed differentially expressed genes (DEGs) of epigenetic chromatin modification enzymes in RG-SCNT, IVF and FF-SCNT embryos of 4cll stage. (E) DEGs of epigenetic chromatin modification enzymes were more than 2-fold higher expression in RG-SCNT and IVF 4cell embryos. (F) DEGs of epigenetic chromatin modification enzymes had more than 2-fold lower expression in in RG-SCNT and IVF 4cell embryos. RG-SCNT, RG108-FFs somatic cell nuclear transfer; FF-SCNT, FFs somatic cell nuclear transfer. Data presented as the mean ¡À standard deviation. *, P <0.05; **, P <0.01, as indicated.

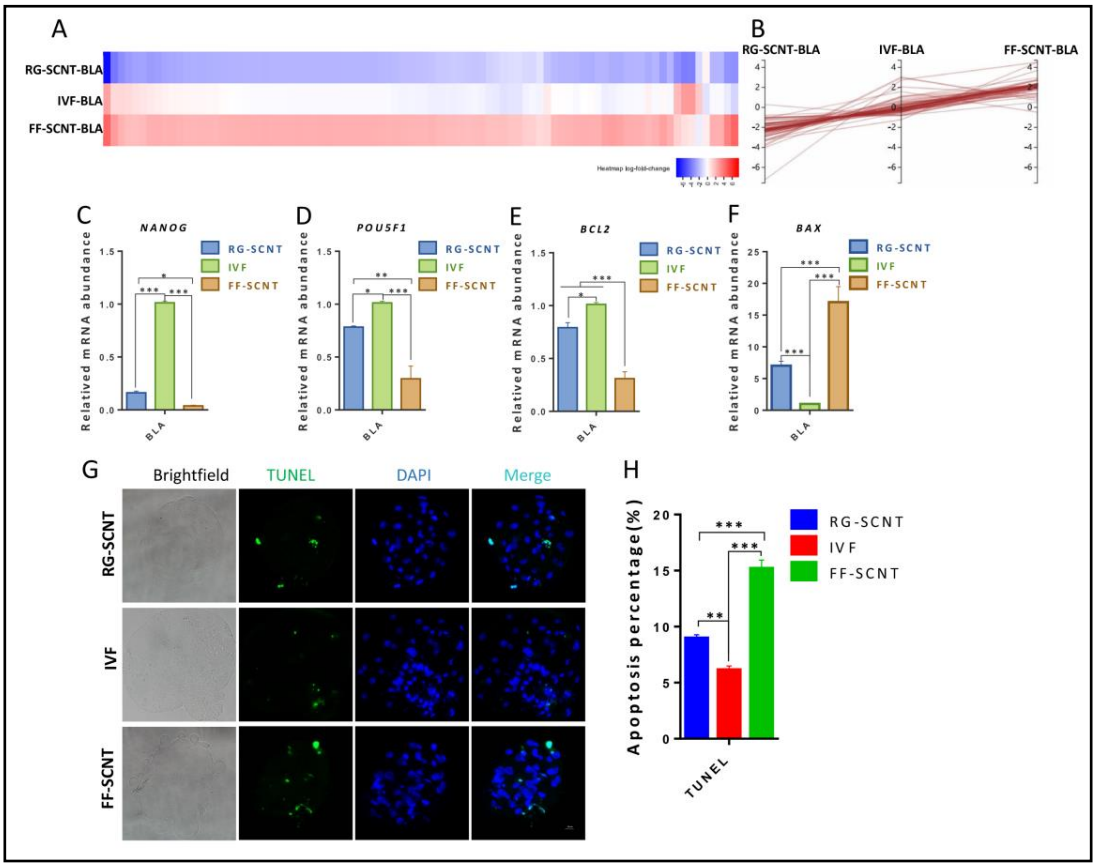

Fig. 9. RG108 improved the developmental capacity and quality of embryos. (A-B) Parallel coordinate plots and heat map illustration of DEGs of epigenetic chromatin-modification enzymes at blastocyst stage derived from RG-SCNT, IVF and FF-SCNT embryos. Abs log FC >1, FDR cut-off <0.05. Relative abundance of the pluripotency genes NANOG (C), POU5F1 (D) and apoptosis-related genes BCL2 (E), BAX (F) transcript in porcine RG-SCNT, IVF and FF-SCNT blastocysts. Quantities were normalized to GAPDH abundance. (G and H) Apoptosis in the FF-SCNT, IVF and FF-SCNT blastocysts. (G) Representative examples of fragmented nuclei (green), which are indicative of apoptosis, versus total nuclei (blue). Scale bar, 25 ¦Ìm. (H) Percentage of apoptotic cells in blastocysts per groups. BLA, blastocysts; RG-SCNT, RG108-FFs somatic cell nuclear transfer; FF-SCNT, FFs somatic cell nuclear transfer. Data presented as the mean ¡À standard deviation. *, P <0.05; **, P <0.01 between groups, as indicated.

AURKA, *HAT1*, *ESCO*$_2$ and *LOC100512284*). All 9 genes had P-values <0.05 or smaller (Fig. 8D and 8F). Overall, 18 of the 28 differentially expressed genes (DEGs) promoted the epigenetic reprogramming. This confirmed that there were abnormal expression patterns of epigenetic modification enzymes in porcine FF-SCNT-4C embryos involved in a variety of epigenetic modifications which were likely to caused abnormal ZGA, and RG108 partially rescued the incorrect epigenetic modifications and promoted to breakthrough the development arrest.

RG108 improved the quality of cloned blastocysts

We also found that RG108 had some influence on the abnormal epigenetic modification in the blastocysts. Thus, we performed a pig epigenetic chromatin modification enzymes RT^2 profiler PCR array in IVF blastocysts (IVF-BLA), FF-SCNT blastocyst (FF-SCNT-BLA) and RG-SCNT blastocyst (RG-SCNT-BLA) embryos. Using the IVF fertilized embryos as a positive control, the results showed that compared with the FF-SCNT blastocyst, most of the abnormal expression of chromatin modification enzymes were rescued in RG-SCNT blastocysts (Fig. 9A and 9B). The expression levels of the pluripotency genes *NANOG* and *POU5F1* and the apoptosis-related genes *BCL2* were significantly higher in the RG-SCNT embryos than those

in the FF-SCNT embryos but still lower than in the IVF blastocysts (Fig. 9C, 9D and 9E). The expression of *BAX* in the RG-SCNT embryos was significantly lower than that in the FF-SCNT embryos. Compared with the IVF embryos, the BAX expression in both SCNT embryos was significantly increased (Fig. 9F). The IVF blastocyst (55.12±3.41) and RG-SCNT blastocysts (47.67±2.45) had higher numbers of total cells than the FF-SCNT (39.33±0.88) blastocysts (Table 5). Apoptotic staining in the Day-7 blastocysts showed that the apoptotic rate of RG-SCNT blastocysts was significantly lower than that in the FF-SCNT blastocysts, but still higher than in the IVF blastocysts (Fig. 9G and 9H). These results suggested that RG108 improved the development and quality of blastocyst by inhibiting apoptosis.

Discussion

It has been reported that many different epigenetic modifications can change the structure of chromatin and participate in the regulation of gene expression and nuclear reprogramming during SCNT [26, 27]. However, there is no clear consensus about how the DNA methylation pattern linked to the histone modifications and how the complex epigenetic information is integrated and translated into defined chromatin structures and gene expression level. Nebendahl *et al.* found that improving the level of H3K9Ac in pig donor cells by reconstructing a de-polymerization of chromatin properties increased the developmental efficiency of SCNT embryos [28]. It has been reported that epigenetic regulators that bind DNA and histone marks are ideally suited to link the intramolecular interactions between different binding domains and may contribute to specific gene expression and epigenetic regulation [29]. In this study, we investigated the mechanism whereby the epigenomic status of donor cells affected SCNT embryo development and the crosstalk between epigenetic signals by using RG108, a DNMT inhibitor.

DNA methylation has been reported to regulate the basic DNA sequence transcription potential in pigs and mice by changing the chromatin density and DNA accessibility to the cytoplasm [30-32]. The abnormal expression of *DNMTs* in donor cells results in DNA methylation defects and aberrant embryo development in pigs [33]. Piccolo *et al.* reported that *TET1* and *TET2* respectively mediate the demethylation of imprinted genes and pluripotent genes, respectively, during reprogramming [34]. In our work, RG108 was employed to regulate the DNA methylation status of FFs, which could be incorporated into the genome during DNA synthesis and to analyze the dynamic expression of DNA methylation related genes and the global DNA methylation expression level of preimplantation embryos. Our results showed that DNA demethylation was enhanced by the significantly improving expression of *TET1*, *TET2* and *TET3* and the remarkable inhibition expression of *DNMT1* and *DNMT3A* in RG108-FFs and also in the RG-SCNT embryos. *CENREP* maintained moderate DNA methylation level. Partial DNA demethylation appeared in the 4-cell stage in RG-SCNT embryo but was not statistically significant. The steady DNA methylation in *CENREP* benefits for maintaining the chromatin stability. Meanwhile, the 5hmC levels were significantly increased in RG-SCNT embryos, and the DNA methylation level in the *NANOG* and *POU5F1* promoter regions were significantly decreased, which resulted in increasing the global DNA methylation levels, activating pluripotent genes expression and reconstructing histone modification. These results indicated that RG108 could effectively reduce the DNA methylation level of FFs, promote active DNA demethylation and passive DNA demethylation, change the expression patterns of *DNMTs* and *TETs*, and activate the pluripotent genes expression in RG-SCNT embryos.

In addition to DNA methylation, histone modification is also an important epigenetic modification during SCNT embryo development. It has long been postulated that the histones directly participate in many different cDNA-template programmes including transcription, replication, recombination and DNA repair [35]. The indirect transcriptional silencing effect of DNA methylation has been reported to be mediated by recruiting active deacetylase complexes (*HDAC1* and *HDAC2*) [36, 37]. It has also been shown that the transcriptional levels

of *TET1*, *TET2*, and *TET3* are increased by knockdown of *KDM5B*, which indicates crosstalk between histone modifications and DNA methylation [38]. To further clarify the potential mechanisms of epigenetic interplay between DNA methylation and histone modifications, we performed epigenetic chromatin modification enzymes RT^2 Profiler PCR Arrays and detected the dynamic reprogramming of histone H3K4 and H3K9 modifications. Our results showed that H3K4 specific histone methyltransferase enzymes were higher expression and H3K9 and H3K27 specific histone methyltransferase enzymes were lower expression in RG108-FFs. The signal intensity of active modification of H3K4me3 and H3K9Ac was significantly increased and the signal intensity of inhibitory modification H3K9me3 were significantly decreased in RG108-FFs and in RG-SCNT 4-cell embryos. These results indicated that reducing the DNA methylation levels by RG108 could effectively improve the expression pattern of H3K4me3, H3K9Ac and H3K9me3 in RG108-FFs and RG-SCNT embryos, which may accelerate reprogramming of the fetal fibroblasts genome and promote the expression of transcriptional activation enzyme associated with histone H3K4 methyltransferase.

In early mammalian embryos, the genome is transcriptionally quiescent until the ZGA [39] and incomplete ZGA has been confirmed to exist in mouse and human SCNT embryos, leading to poor developmental potential [40, 41]. Cao *et al.* found that ZGA of porcine fertilized embryos occurred at the 4cell stage in porcine fertilized embryos and was delayed in SCNT embryos via genome-wide gene expression analysis [42], but, a comprehensive analysis of global epigenetic modification of porcine preimplantation embryos has not previously been conducted. Previous studies characterized and compared dynamic genome-wide profiles of 12 kinds of histone methylation modification by IF staining [43], but no studies have been conducted on dynamic mRNA profiling of global epigenetic modification enzymes. In our study, we conducted an overall analysis of the expression profiles of 84 representative chromatin modification enzymes by means of RT^2 Profiler PCR arrays. We used IVF embryos as a positive control and the results showed that some of the abnormal expression of chromatin modification enzymes were rescued in RG-SCNT embryos. The cluster analysis showed that the expression pattern of 84 epigenetic chromatin modification enzymes in RG-SCNT embryos were closer to that of the IVF embryos. Nineteen chromatin-modified enzymes in the IVF and RG-SCNT embryos had significantly higher expression than in the FF-SCNT embryos, and these highly expressed enzymes were mainly associated with transcriptional activation, including histone methyltransferase (H3K4 specific), histone acetyltransferase, ubiquitin conjugating enzyme and nuclear receptor coactivator. Moreover, 9 kinds of modification enzymes had significantly lower expression in RG-SCNT embryos than in FF-SCNT embryos, some of which were associated with transcriptional inhibition. Among these, 18 of the 28 differentially expressed chromatin modification enzymes functioned to improve transcriptional activation and facilitating normal epigenetic reprogramming. These results indicated that there was a positive correlation between promoting the expression of transcriptional activation enzymes, mainly including H3K4 specific histone methyltransferase, and restoring the abnormal epigenetic reprogramming during the ZGA.

It has been reported that DNA methylation and histone modifications are key epigenetic modifications of chromatin and widely regulate gene transcription expression and silencing [44, 45]. The disruption of histone modifications causes defective chromosome condensation and segregation, delayed embryo development progression [46, 47]. In our study, we found that the epigenetic reprogramming of 5hmC, H3K9Ac and H3K9me3 in RG-SCNT embryos at the blastocyst stage were improved when compared with FF-SCNT. Meanwhile, we found that the expression level of *BCL2* was increased and the *BAX* was decreased, which inhibited the apoptosis process. These changes in epigenetic modifications and genes expression response to apoptosis changes. The results indicated that reconstructing normal epigenetic modifications in blastocysts had a positive correlation with inhibiting the apoptosis process, which were conducive to improving the quality of blastocysts.

Conclusion

In conclusion, dynamic changes of DNA methylation by RG108 result in epigenetic reprogramming of H3K4me3, H3K9Ac and H3K9me3, which leads to the activation of the zygotic genome and transcriptional-related enzymes associated with H3K4 methylation, and contributes to reconstructing normal epigenetic modifications and improving the developmental efficiency of porcine SCNT embryos.

Acknowledgements

This work was supported by National Key R&D Program of China (No: 2017YFA0104400), Program for Changjiang Scholars and Innovative Research Team in University (PCSIRT, No. IRT_16R32) and Program for JLU Science and Technology Innovative Research Team (JLUSTIRT).

Disclosure Statement

The authors declare that there is no conflict of interest that could be perceived as prejudicing the impartiality of the research reported.

References

1 Han YM, Kang YK, Koo DB, Lee KK: Nuclear reprogramming of cloned embryos produced *in vitro*. Theriogenology 2003;59:33-44.
2 Ao Z, Liu DW, Cai GY, Wu ZF, Li ZC: [Placental developmental defects in cloned mammalian animals]. Yi Chuan 2016;38:402-410.
3 Hochedlinger K, Jaenisch R: Monoclonal mice generated by nuclear transfer from mature B and T donor cells. Nature 2002;415:1035-1038.
4 Bird A: DNA methylation patterns and epigenetic memory. Genes Dev 2002;16:6-21.
5 Mutskov VJ, Farrell CM, Wade PA, Wolffe AP, Felsenfeld G: The barrier function of an insulator couples high histone acetylation levels with specific protection of promoter DNA from methylation. Genes Dev 2002;16:1540-1554.
6 Dannenberg LO, Edenberg HJ: Epigenetics of gene expression in human hepatoma cells: expression profiling the response to inhibition of DNA methylation and histone deacetylation. BMC Genomics 2006;7:181.
7 Lai L, Huan Y, Wu Z, Zhang J, Zhu J, Liu Z, Song X: Epigenetic Modification Agents Improve Gene-Specific Methylation Reprogramming in Porcine Cloned Embryos. Plos One 2015;10:e0129803.
8 Fouse SD, Shen Y, Pellegrini M, Cole S, Meissner A, Van Neste L, Jaenisch R, Fan G: Promoter CpG methylation contributes to ES cell gene regulation in parallel with Oct4/Nanog, PcG complex, and histone H3 K4/K27 trimethylation. Cell Stem Cell 2008;2:160-169.
9 Bird A: Perceptions of epigenetics. Nature 2007;447:396-398.
10 Brueckner B, Garcia Boy R, Siedlecki P, Musch T, Kliem HC, Zielenkiewicz P, Suhai S, Wiessler M, Lyko F: Epigenetic reactivation of tumor suppressor genes by a novel small-molecule inhibitor of human DNA methyltransferases. Cancer Res 2005;65:6305-6311.
11 Stresemann C, Brueckner B, Musch T, Stopper H, Lyko F: Functional diversity of DNA methyltransferase inhibitors in human cancer cell lines. Cancer Res 2006;66:2794-2800.
12 Saini M, Selokar NL, Agrawal H, Singla SK, Chauhan MS, Manik RS, Palta P: Treatment of Donor Cells and Reconstructed Embryos with a Combination of Trichostatin-A and 5-aza-2'-Deoxycytidine Improves the Developmental Competence and Quality of Buffalo Embryos Produced by Handmade Cloning and Alters Their Epigenetic Status and Gene Expression. Cell Reprogram 2017;19:208-215.

13 Cheng JC, Matsen CB, Gonzales FA, Ye W, Greer S, Marquez VE, Jones PA, Selker EU: Inhibition of DNA methylation and reactivation of silenced genes by zebularine. J Natl Cancer Inst 2003;95:399-409.
14 Sun HL, Meng LN, Zhao X, Jiang JR, Liu QY, Shi DS, Lu FH: Effects of DNA methyltransferase inhibitor RG108 on methylation in buffalo adult fibroblasts and subsequent embryonic development following somatic cell nuclear transfer. Genet Mol Res 2016;15.
15 Diao YF, Naruse KJ, Han RX, Li XX, Oqani RK, Lin T, Jin DI: Treatment of fetal fibroblasts with DNA methylation inhibitors and/or histone deacetylase inhibitors improves the development of porcine nuclear transfer-derived embryos. Anim Reprod Sci 2013;141:164-171.
16 Li M, Li YH, Hou Y, Sun XF, Sun Q, Wang WH: Isolation and culture of pluripotent cells from *in vitro* produced porcine embryos. Zygote 2004;12:43-48.
17 Brevini TA, Antonini S, Cillo F, Crestan M, Gandolfi F: Porcine embryonic stem cells: Facts, challenges and hopes. Theriogenology 2007;68 Suppl 1:S206-213.
18 Hall V: Porcine embryonic stem cells: a possible source for cell replacement therapy. Stem Cell Rev 2008;4:275-282.
19 Kim S, Kim JH, Lee E, Jeong YW, Hossein MS, Park SM, Park SW, Lee JY, Jeong YI, Kim HS, Kim YW, Hyun SH, Hwang WS: Establishment and characterization of embryonic stem-like cells from porcine somatic cell nuclear transfer blastocysts. Zygote 2010;18:93-101.
20 Amouroux R, Nashun B, Shirane K, Nakagawa S, Hill PW, D'Souza Z, Nakayama M, Matsuda M, Turp A, Ndjetehe E, Encheva V, Kudo NR, Koseki H, Sasaki H, Hajkova P: De novo DNA methylation drives 5hmC accumulation in mouse zygotes. Nat Cell Biol 2016;18:225-233.
21 Livak KJ, Schmittgen TD: Analysis of relative gene expression data using real-time quantitative PCR and the 2(-Delta Delta C(T)) Method. Methods 2001;25:402-408.
22 Goolam M, Scialdone A, Graham SJL, Macaulay IC, Jedrusik A, Hupalowska A, Voet T, Marioni JC, Zernicka-Goetz M: Heterogeneity in Oct4 and Sox2 Targets Biases Cell Fate in 4-Cell Mouse Embryos. Cell 2016;165:61-74.
23 Ritchie ME, Phipson B, Wu D, Hu Y, Law CW, Shi W, Smyth GK: limma powers differential expression analyses for RNA-sequencing and microarray studies. Nucleic Acids Res 2015;43:e47.
24 Perez-Llamas C, Lopez-Bigas N: Gitools: analysis and visualisation of genomic data using interactive heat-maps. PLoS One 2011;6:e19541.
25 Jones PA: Functions of DNA methylation: islands, start sites, gene bodies and beyond. Nat Rev Genet 2012;13:484-492.
26 Xu Q, Xie W: Epigenome in Early Mammalian Development: Inheritance, Reprogramming and Establishment. Trends Cell Biol 2017.
27 Glanzner WG, Wachter A, Coutinho AR, Albornoz MS, Duggavathi R, Gon CPB, Bordignon V: Altered expression of BRG1 and histone demethylases, and aberrant H3K4 methylation in less developmentally competent embryos at the time of embryonic genome activation. Mol Reprod Dev 2017;84:19-29.
28 Nebendahl C, Gors S, Albrecht E, Kruger R, Martens K, Giller K, Hammon HM, Rimbach G, Metges CC: Early postnatal feed restriction reduces liver connective tissue levels and affects H3K9 acetylation state of regulated genes associated with protein metabolism in low birth weight pigs. J Nutr Biochem 2016;29:41-55.
29 Hashimoto H, Horton JR, Zhang X, Cheng X: UHRF1, a modular multi-domain protein, regulates replication-coupled crosstalk between DNA methylation and histone modifications. Epigenetics 2009;4:8-14.
30 Arai Y, Umeyama K, Takeuchi K, Okazaki N, Hichiwa N, Yashima S, Nakano K, Nagashima H, Ohgane J: Establishment of DNA methylation patterns of the Fibrillin1 (FBN1) gene in porcine embryos and tissues. J Reprod Dev 2017.
31 Cedar H, Bergman Y: Linking DNA methylation and histone modification: patterns and paradigms. Nat Rev Genet 2009;10:295-304.
32 Straussman R, Nejman D, Roberts D, Steinfeld I, Blum B, Benvenisty N, Simon I, Yakhini Z, Cedar H: Developmental programming of CpG island methylation profiles in the human genome. Nat Struct Mol Biol 2009;16:564-571.
33 Song X, Liu Z, He H, Wang J, Li H, Li J, Li F, Jiang Z, Huan Y: Dnmt1s in donor cells is a barrier to SCNT-mediated DNA methylation reprogramming in pigs. Oncotarget 2017.
34 Piccolo FM, Fisher AG: Getting rid of DNA methylation. Trends Cell Biol 2014;24:136-143.

35 Luger K, Mader AW, Richmond RK, Sargent DF, Richmond TJ: Crystal structure of the nucleosome core particle at 2.8 A resolution. Nature 1997;389:251-260.
36 Nan X, Ng HH, Johnson CA, Laherty CD, Turner BM, Eisenman RN, Bird A: Transcriptional repression by the methyl-CpG-binding protein MeCP2 involves a histone deacetylase complex. Nature 1998;393:386-389.
37 Meehan RR, Lewis JD, Bird AP: Characterization of MeCP2, a vertebrate DNA binding protein with affinity for methylated DNA. Nucleic Acids Res 1992;20:5085-5092.
38 Huang J, Zhang H, Wang X, Dobbs KB, Yao J, Qin G, Whitworth K, Walters EM, Prather RS, Zhao J: Impairment of preimplantation porcine embryo development by histone demethylase KDM5B knockdown through disturbance of bivalent H3K4me3-H3K27me3 modifications. Biol Reprod 2015;92:72.
39 Yu C, Ji SY, Dang YJ, Sha QQ, Yuan YF, Zhou JJ, Yan LY, Qiao J, Tang F, Fan HY: Oocyte-expressed yes-associated protein is a key activator of the early zygotic genome in mouse. Cell Res 2016;26:275-287.
40 Zheng H, Huang B, Zhang B, Xiang Y, Du Z, Xu Q, Li Y, Wang Q, Ma J, Peng X, Xu F, Xie W: Resetting Epigenetic Memory by Reprogramming of Histone Modifications in Mammals. Mol Cell 2016;63:1066-1079.
41 Chung YG, Matoba S, Liu Y, Eum JH, Lu F, Jiang W, Lee JE, Sepilian V, Cha KY, Lee DR, Zhang Y: Histone Demethylase Expression Enhances Human Somatic Cell Nuclear Transfer Efficiency and Promotes Derivation of Pluripotent Stem Cells. Cell Stem Cell 2015;17:758-766.
42 Cao S, Han J, Wu J, Li Q, Liu S, Zhang W, Pei Y, Ruan X, Liu Z, Wang X, Lim B, Li N: Specific gene-regulation networks during the pre-implantation development of the pig embryo as revealed by deep sequencing. BMC Genomics 2014;15:4.
43 Cao Z, Li Y, Chen Z, Wang H, Zhang M, Zhou N, Wu R, Ling Y, Fang F, Li N, Zhang Y: Genome-Wide Dynamic Profiling of Histone Methylation during Nuclear Transfer-Mediated Porcine Somatic Cell Reprogramming. PLoS One 2015;10:e0144897.
44 Zhang L, Xie WJ, Liu S, Meng L, Gu C, Gao YQ: DNA Methylation Landscape Reflects the Spatial Organization of Chromatin in Different Cells. Biophys J 2017;113:1395-1404.
45 Samson M, Jow MM, Wong CC, Fitzpatrick C, Aslanian A, Saucedo I, Estrada R, Ito T, Park SK, Yates JR, 3rd, Chu DS: The specification and global reprogramming of histone epigenetic marks during gamete formation and early embryo development in C. elegans. PLoS Genet 2014;10:e1004588.
46 Xu D, Bai J, Duan Q, Costa M, Dai W: Covalent modifications of histones during mitosis and meiosis. Cell Cycle 2009;8:3688-3694.
47 Qian Y, Tu J, Tang NL, Kong GW, Chung JP, Chan WY, Lee TL: Dynamic changes of DNA epigenetic marks in mouse oocytes during natural and accelerated aging. Int J Biochem Cell Biol 2015;67:121-127.